

ARTICLE

Danilo Milardi · Carmelo La Rosa · Domenico Grasso
Rita Guzzi · Luigi Sportelli · Carlo Fini

Thermodynamics and kinetics of the thermal unfolding of plastocyanin

Received: 17 July 1997 / Revised version: 22 November 1997 / Accepted: 15 January 1998

Abstract The thermal denaturation of plastocyanin in aqueous solution was investigated by means of DSC, ESR and absorbance techniques, with the aim of determining the thermodynamic stability of the protein and of characterizing the thermally induced conformational changes of its active site. The DSC and absorbance experiments indicated an irreversible and kinetically controlled denaturation path. The extrapolation of the heat capacity and optical data at infinite scan rate made it possible to calculate the kinetic and thermodynamic parameters associated with the denaturation steps. The denaturation pathway proposed, and the parameters found from the calorimetric data, were checked by computer simulation using an equation containing the information necessary to describe the denaturation process in detail. ESR and absorbance measurements have shown that structural changes of the copper environment occur during the protein denaturation. In particular, the geometry of the copper-ligand atoms changes from being tetrahedral to square planar and the disruption of the active site precedes the global protein denaturation. The thermodynamic enthalpic change, the half-width transition temperature, and the value of ΔC_p , were used to calculate the thermodynamic stability, ΔG , of the reversible process over the entire temperature range of denaturation. The low thermal stability found for plastocyanin, is discussed in connection with structural factors stabilizing the native state of a protein.

Key words Plastocyanin · Unfolding · Thermodynamics

Based on a presentation at the 2nd European Biophysics Congress, Orléans, France, July 1997.

D. Milardi · C. La Rosa · D. Grasso (✉)
Dipartimento di Scienze Chimiche,
Università di Catania Via del le A. Doria 6, I-95125 Catania, Italy

R. Guzzi · L. Sportelli
Dipartimento di Fisica, Università della Calabria and Unità INFM,
and Unità INFM, I-87036 Arcavacata di Rende, Cosenza, Italy

C. Fini
Dipartimento di Biologia Cellulare e Molecolare, and Unità INFM,
Università di Perugia, Via del Giochetto, I-06126, Perugia, Italy

Abbreviations PC Plastocyanin · DSC Differential scanning calorimetry · ESR Electron spin resonance · OD Optical density

Introduction

Plastocyanin (PC) is a 10.5 kDa blue copper protein which functions in the electron transport chain of chloroplasts (Sykes 1985; Redimbo et al. 1994). Together with azurin, this protein is one of the best characterized of this class (Colman et al. 1978; Adam 1985; Sykes 1991; Guss et al. 1992). It contains a single copper atom, which is coordinated to two N atoms (His-37, His-87) and two S atoms (Cys-84, Met-92) in a distorted tetrahedral geometry (Guss and Freeman 1983; Guss et al. 1986; Chazin and Wright 1988; Redimbo et al. 1994). The distorted geometry of the copper center is responsible for the intense blue color of the oxidized form of the protein, for its high redox potential (Sanderson et al. 1986; Gray and Solomon 1981) and for its magnetic properties (Redimbo et al. 1994). It has been shown that the copper center plays a crucial role in stabilizing the native conformation of the PC molecule (Merchant and Bogorad 1986a, b). More recent studies also suggest that the influence of the copper oxidation state on the thermal stability of PC (Gross et al. 1992) should not be ignored. However, to the best of our knowledge, no thermodynamic data on the thermal denaturation of PC are currently available in the literature.

In this paper we have investigated the thermal behaviour of PC using DSC, absorbance and EPR spectroscopy. The thermodynamic parameters were evaluated by DSC measurements (Privalov and Khechinashvili 1974). Unfortunately, the thermal denaturation of PC is, on the whole, an irreversible process, so that statistical-mechanical deconvolution methods (Freire and Biltonen 1978) and classical thermodynamic analysis cannot be applied (Edge et al. 1985). In addition, the remarkable asymmetry of the DSC curves at the end of the thermal transition, ascribable to exothermic phenomena as well as to the occurrence of

kinetic factors, is a further complication in the analysis of the PC unfolding process (Freire et al. 1990; Galisteo and Sanchez-Ruiz 1993).

However, we use a mathematical extrapolation procedure (Freire et al. 1990; La Rosa et al. 1995) to separate the reversible step of the denaturation process from the irreversible one. The extrapolated parameters related to the reversible step are subsequently used to simulate the $C_{p_{exc}}$ profiles by means of a best-fit program using the SIMPLEX minimisation algorithm. This algorithm is based on a previously developed equation, which works on the basis of the hypothesized pathway of denaturation (Milardi et al. 1994). The model proposed describes very well the denaturation path of PC as the sum of two effects: an endothermic effect comprising the energy involved in the melting of the protein's three-dimensional structure, and an exothermic effect ascribable to the aggregation of the polypeptide chain. The first of these effects is, as will be explained, reversible and in this case thermodynamic analysis is allowed. In contrast, the second effect is irreversible, kinetically controlled and slower than the reversible unfolding process.

The spectroscopic features of the active site of the oxidized form of PC, i.e. the intense optical charge transfer (CT) transition at $\lambda_{max} = 597$ nm and the small value of the parallel component of the hyperfine coupling tensor of the copper ion (Gewirth and Solomon 1988; Adman 1993), make this protein a suitable system to compare the thermal properties of the whole macromolecule with the conformational transitions occurring in the copper environment as the temperature increases. In fact, since the copper-ligand atoms are located in different portions of the β -sheets, any significant changes in the secondary or tertiary structure would be expected to alter the properties of the copper center. Within this framework, both absorbance and DSC measurements were carried out under the same experimental conditions. The results show that the overall protein denaturation occurs after the disruption of the active site and that during the thermal transition the geometry of the copper site changes from tetrahedral, in the native state, to square planar, in the denaturated state, where the substitution of the sulfur atoms probably occurs.

Materials and methods

Chemicals

PC was isolated from spinach chloroplasts as reported elsewhere (Wang et al. 1986). The A_{597}/A_{280} absorption ratio measured at room temperature was 0.51. Protein concentration was checked spectrophotometrically at room temperature using a molar extinction coefficient of $\epsilon_{597} = 4900 \text{ M}^{-1} \text{ cm}^{-1}$ (Gross et al. 1992). Potassium phosphate (analytical grade) was obtained from Fluka Chemie AG (Buchs, Switzerland). Phosphate buffer solution, 10 mM, pH = 7.03, was used in all experiments. The ionic strength was adjusted to 0.1 with sodium chloride.

Differential scanning calorimetry

DSC scans were carried out with a third-generation SET-ARAM (Lyon, France) micro differential scanning calorimeter (microDSCIII) with stainless steel 1 ml sample cells, interfaced with a computer. Both the sample (0.94 mg/ml in PC) and reference (buffer without the protein) cells were scanned from 25 to 100 °C with a precision of ± 0.02 °C, at scanning rates of 0.3, 0.5, 0.7 and 1.0 °C/min. In order to obtain the C_p curves, buffer-buffer base lines were obtained at the same scanning rate and then subtracted from sample curves (Sturtevant 1987; Connelly et al. 1991). All the $C_{p_{exc}}$ curves were obtained using a fourth-order polynomial fit as baseline as reported in Fig. 1. The average level of noise was about $\pm 0.4 \mu\text{W}$ and the reproducibility at refilling was, under the adopted experimental conditions, about 0.1 mJ/K/ml.

Calibration in energy was obtained by providing a definite power supply, electrically generated by an EJ2 SET-ARAM Joule calibrator within the sample cell.

Optical density

Absorbance measurements were carried out with a JASCO 7850 spectrophotometer equipped with a model TPU-436 Peltier type thermostatted cell holder and a model EHC-441 temperature programmer (precision ± 0.02 °C). The scanning rates were the same as used for the DSC measurements. Quartz cuvettes with a 1 cm optical path were used throughout. Protein concentration was 3×10^{-5} M. Measurements were begun 3 minutes after positioning the samples in the thermostatted sample holder at the initial temperature of 35 °C. The temperature of the sample was measured directly by a YSI precision thermistor dip in the reference cuvette. The temperature of the optical transition, T_t , is defined as the midpoint of the absorbance profile.

The kinetics of the thermal denaturation of PC were studied by following the time-dependent OD_{597} variation at fixed temperatures $T \leq T_t$. The first-order rate constants (k) of the thermal denaturation of PC were obtained as reported elsewhere (Guzzi et al. 1996) and used to calculate the apparent activation energy, E_a .

Electron spin resonance

EPR measurements were carried out with a Bruker ER 200D-SRC X band spectrometer equipped with the ESP 1600 Data System. The EPR spectra of the native and denaturated samples of PC were recorded at 77 K by plunging the sample solution in a finger dewar containing liquid nitrogen. Protein concentration was 5×10^{-4} M. The $g_{||}$ component of the axial symmetric g tensor and the $A_{||}$ component of the hyperfine tensor A were extracted from the EPR spectra. These two magnetic parameters provide information about the geometry and the ligand atoms of the copper ion in PC.

It is worthwhile to point out that the different experimental techniques used required a different protein concentration in order to obtain an acceptable signal-to noise ratio. However, no concentration dependence of the experimental data was observed. Repeating each experiment at least three times tested the reproducibility of all the experimental data.

Results

Figure 1 shows the calorimetric profile of PC in aqueous solution recorded at 0.5 °C/min in the 40–95 °C temperature range. The temperature of maximum heat absorption, T_m , is 68.44 °C. No calorimetric reversibility was observed, i.e. no endothermic peak appears during a second run of a previously scanned sample. The same behavior was also observed when the protein is heated a few degrees beyond the apparent T_m , cooled and re-heated. This means that the thermal denaturation of PC is, on the whole, an irreversible process and it cannot be directly analysed using classical thermodynamics. On the other hand, the van't Hoff ratio $\Delta H_{cal}/\Delta H_{vH}=2.7$ (Table 1), suggests that the thermal transition of PC cannot be described in terms of

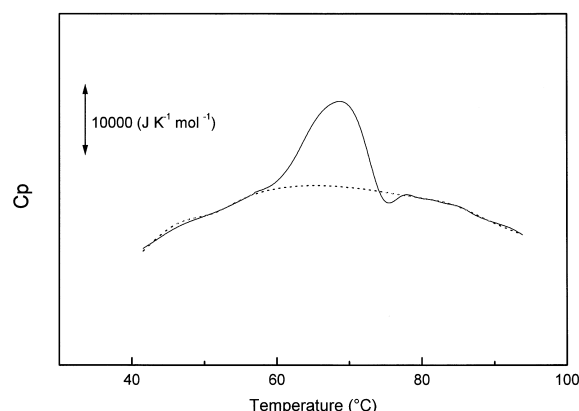


Fig. 1 DSC thermogram of PC after subtraction of the buffer-buffer base line. Protein concentration 0.94 mg/ml, pH=7.03, ionic strength 0.1 in NaCl, scan rate 0.5 °C/min. The baseline (dashed line) was obtained as described in the text

Table 1 Scanning rate effect on the thermal denaturation of plastocyanin in aqueous solution obtained at constant protein concentration. pH and ionic strength were 7.03 and 0.1 in NaCl, respectively

Scan/rate (°C/min)	OD T_t (°C) ^a	DSC T_m (°C) ^a	ΔH (kJ/mole) ^a	$\Delta H_{cal}/$ ΔH_{vH}
0.3	58.34 ± 0.03	68.03 ± 0.05	98 ± 20	5.0
0.5	61.00 ± 0.08	68.44 ± 0.04	140 ± 22	2.7
0.7	61.47 ± 0.06	70.65 ± 0.03	179 ± 29	2.0
1.0	63.50 ± 0.03	70.54 ± 0.05	194 ± 21	1.4

* Values obtained by extrapolation as reported in the text

^a Values expressed as mean ± standard deviation

the “two-state” model (Privalov and Potekhin 1986; Dill and Shortle 1991). Since the transition is irreversible, it was necessary to establish if the reaction was under kinetic control and if a change of molecularity or association/dissociation took place during the heating of the protein solution (Sanchez-Ruiz 1992). DSC profiles at different scan rates allowed us to determine if the process was under kinetic control. A change of molecularity with heating was not evident because DSC profiles of PC do not depend on protein concentration (data not shown) (Sanchez-Ruiz 1992; Sanchez-Ruiz et al. 1988; La Rosa et al. 1995).

Scanning rate effect on DSC thermograms

Figure 2 shows the DSC profiles of PC in aqueous solution obtained at 0.3, 0.5, 0.7 and 1.0 °C/min. From the scanning rate effect, the apparent activation energy, E_{app} , of the denaturation process can be calculated using the following equation (Sanchez-Ruiz 1992; Sanchez-Ruiz et al. 1988):

$$\ln(v/T_m^2 C) = C - E_{app}/(RT_m) \quad (1)$$

where v is the scan rate (°C/min) and C is a constant. The slope of the linear plot of $\ln(v/T_m^2)$ vs. $1/T_m$, gives the E_{app} of the process ($E_{app} = 322 \pm 27$ kJ/mol). From Fig. 2, it can also be noted that the amplitude of the exothermic peak, localised at the end of the transition, diminishes when the scan rate increases, while calorimetric enthalpy, ΔH , and T_m increase with increasing scan rates (Table 1).

The scan rate influences the exothermic and endothermic phenomena differently (Milardi et al. 1994). Even if both peaks become sharper and shift towards the low temperature side when v decreases, this effect is much greater for the exothermic peak than for the endothermic one.

The amplitude reduction of the exothermic peak with increasing scan rate indicates that the exothermic contribution is time-dependent. It is therefore reasonable to consider the reversible and irreversible steps as being separa-

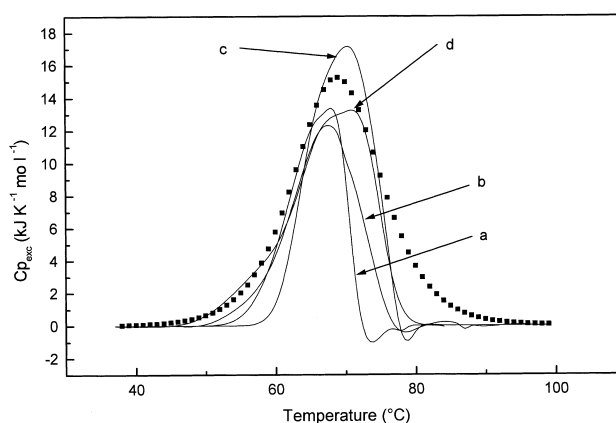


Fig. 2 Effect of scanning rate on the excess heat capacity function of plastocyanin: a 0.3 °C/min, b 0.5 °C/min, c 0.7 °C/min, d 1.0 °C/min. Protein concentration was the same (0.94 mg/ml) in all experiments. Full square points (■) represents the extrapolated excess heat capacity function (see text for details)

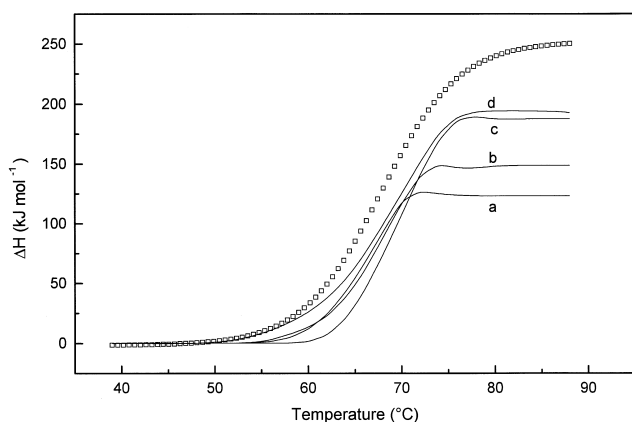


Fig. 3 Cumulative enthalpies obtained at different scan rates *a* 0.3 °C/min, *b* 0.5 °C/min, *c* 0.7 °C/min, *d* 1.0 °C/min. The square points (□) represents the thermodynamic cumulative enthalpy calculated as described in the text at all temperatures within the denaturation range

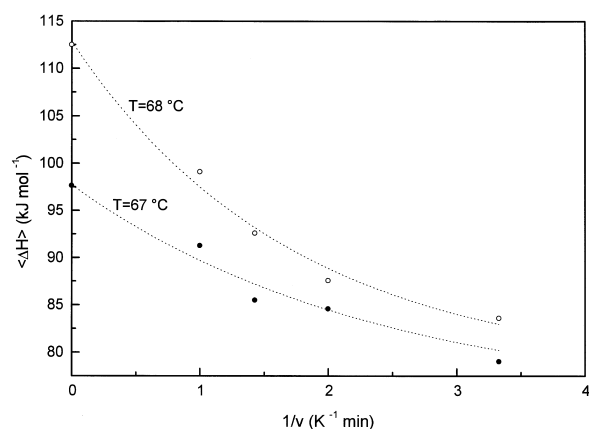


Fig. 4 Examples of exponential plots of the cumulative enthalpies of denaturation $\langle\Delta H\rangle$ vs $1/v$ obtained at $T = 68$ °C (open circles), and $T = 67$ °C (closed circles)

ble through the extrapolation of the calorimetric curves at infinite scanning rates (Freire et al. 1990; Hernandez-Harana 1993; La Rosa et al. 1995).

The $C_{p_{exc}}$ curve at infinite scanning rate was obtained by means of the following procedure: the cumulative enthalpy functions $\langle\Delta H\rangle$ were calculated from the experimental calorimetric profiles obtained at different scan rates by using the following equation:

$$\langle\Delta H\rangle = \int_{T_0}^T C_{p_{exc}} dT \quad (2)$$

where T_0 is the temperature at which all molecules are in the initial state, and $C_{p_{exc}}$ is the molar excess heat calculated according to Privalov and Potekhin (1986) (see Fig. 2).

The $\langle\Delta H\rangle$ profiles depend on the scan rate (Fig. 3), i. e., at each temperature $T = T_i$, where T_i is a temperature within the 40–95 °C range, $\langle\Delta H\rangle$ is a function of the scan rate.

For a first order process, the relationship between $\langle\Delta H\rangle$, $\langle\Delta H\rangle_{rev}$, T and v is given by the following equation (Freire et al. 1990):

$$(\Delta H - \langle\Delta H\rangle) = (\Delta H - \langle\Delta H\rangle_{rev}) \times \exp\left(-\frac{1}{v} \int_{T_0}^T k_{app} dT\right) \quad (3)$$

where ΔH is the calorimetric enthalpy calculated at the chosen scan rate, $\langle\Delta H\rangle_{rev}$ represents the cumulative enthalpy function containing the information pertinent only to the species that are in thermodynamic equilibrium, and k_{app} is the apparent kinetic constant. Obviously, when $v \rightarrow \infty$, $\langle\Delta H\rangle \rightarrow \langle\Delta H\rangle_{rev}$ exponentially.

In order to obtain the $\langle\Delta H\rangle_{rev}$ function over the entire denaturation range, the experimental values of $\langle\Delta H\rangle$ corresponding to the four scan rates are plotted for a given temperature, T_i , vs. $1/v$. In the exponential graphs shown in Fig. 4, the intercept values with the y-axis give the $\langle\Delta H\rangle_{rev}$ values at a given temperature. For the sake of clarity, only the points obtained at $T = 67$ °C and $T = 68$ °C are reported.

Hence, the curve represented by squares (□) in Fig. 3, is made up of all the intercepts obtained as explained above, over the entire denaturation range. By deriving the $\langle\Delta H\rangle_{rev}$ profile with respect to temperature we get the $C_{p_{exc}}$ profile at infinite scanning rate with a $\Delta H = 254$ kJ/mol and a $T_m = 69.0$ °C.

Mechanical-statistical analysis of the time-independent $C_{p_{exc}}$ profile

In order to establish the path of the folding-unfolding transition, a mechanical-statistical analysis of the extrapolated $C_{p_{exc}}$ profile was carried out using the classic deconvolution algorithm of Freire and Biltonen (Freire and Biltonen 1978; Biltonen and Freire 1978). This analysis suggests that the unfolding path of PC is an “all or none” type. The transition, reversible and time-independent, is followed by an irreversible and kinetically controlled step.

OD and EPR results

Figure 5 (solid line) shows the experimental OD_{597} profile of PC in aqueous solution recorded at the scan rate of 0.5 °C/min in the 35 to 75 °C temperature range. The thermal transition of PC is irreversible and occurs at 61 °C. After cooling at room temperature, the initial absorption intensity is no longer detected. The disappearance of the charge-transfer band and the loss of the blue color can be assigned to the temperature-induced conformational changes of the PC tertiary structure, which permanently alter the Cu-S(Cys-84) bond length.

The dependence of the thermal transition of the active site of PC upon scan rate was investigated by taking the OD_{597}/T measurements at 0.3, 0.5, 0.7, 1.0 °C/min. The results, listed in Table 1, show that the optical transition temperature, T_i , increases with the scan rate and suggest that

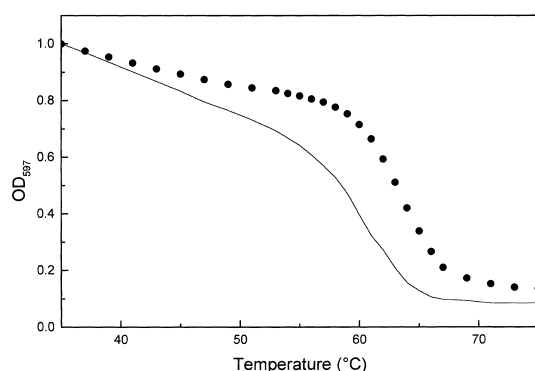


Fig. 5 Normalized OD_{597} variation of PC in aqueous solution as a function of temperature, recorded at $0.5\text{ }^{\circ}\text{C}/\text{min}$ (solid line). Full circles represent the extrapolated OD_{597} variation as a function of temperature

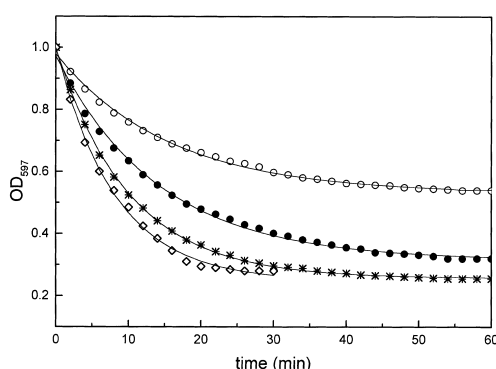


Fig. 6 Normalized OD_{597} /time decay of PC in aqueous solution at (○) 57, (●) 58, (*) 59 and (◇) $61\text{ }^{\circ}\text{C}$. The full lines represent the best fit of the exponential plots

the thermal transition of the active site is an activated process. The results are in good agreement with previous data (Gross et al. 1992). The apparent activation energy, E_a , associated with this process can be calculated from the slope of the linear plot $\ln(v/T_t^2)$ vs. $1/T_t$ and has the value of $174 \pm 31\text{ kJ/mol}$.

Information on the kinetics of the thermal break-up of the copper center can also be obtained by looking at the time-dependence of the optical density at a fixed temperature. In Fig. 6 the normalized OD_{597} /time decay of PC in aqueous solution at temperatures of 57, 58, 59, $61\text{ }^{\circ}\text{C}$ is shown. The solid lines represent the best fit of the experimental points following the procedure described in Guzzi et al. (1996). By using this method an E_a value of $176 \pm 26\text{ kJ/mol}$ was obtained, which corresponds with the value previously found.

The irreversibility of the OD_{597}/T profile in PC prevents the calculation of the thermodynamic parameters related to the process described. However, in some papers concerning the thermal behavior of azurin in aqueous solution (La Rosa et al. 1995; Guzzi et al. 1996) we solved this problem by extracting the reversible contribution to the denaturation process from the irreversible one. Since the de-

naturation path of the two proteins is the same, it is reasonable to extend this procedure to PC. In particular, the OD_{597}/T profile at infinite scan rate was obtained from the four experimental curves recorded at different scan rates. For each temperature $T = T_i$, where $35 < T_i < 75\text{ }^{\circ}\text{C}$, the four OD values were plotted as a function of $1/v$. The experimental points were fitted with a linear function, the intercept with the y-axis giving the OD value at infinite scan rate. The extrapolated OD_{597}/T curve for the reversible process is shown in Fig. 5 (full circles). The apparent enthalpy change, ΔH_{app}^{∞} , was calculated from this profile using the equation (Poklar et al. 1993):

$$\Delta H_{app}^{\infty} = 4 RT_t^{\infty 2} \left(\frac{\partial f_U}{\partial T} \right)_{T=T_t^{\infty}} \quad (4)$$

where T_t^{∞} is the transition temperature of the extrapolated reversible curve, and f_U is:

$$f_U = \frac{OD(T) - OD_N(T)}{OD_U(T) - OD_N(T)} \quad (5)$$

$OD(T)$ is the actual optical density, $OD_N(T)$ and $OD_U(T)$ are the OD values of the native and the unfolded state, respectively. The ΔH_{app}^{∞} and T_t^{∞} values for PC in aqueous solution are $284 \pm 41\text{ kJ/mol}$ and $63.5\text{ }^{\circ}\text{C}$, respectively.

Temperature-induced changes in the copper coordination geometry are also revealed by EPR spectroscopy. This technique, like spectrophotometry, provides local information about the structural modification occurring in the copper environment. However, since the copper center is deeply buried in a hydrophobic region of the protein, conformational transitions occurring in a contiguous region could spread to the copper site and result in altered EPR and optical spectra.

The EPR spectra of native and thermally denaturated samples of PC are shown in Fig. 7. The spectral features of native PC (Fig. 7a) are typical of a type I copper ion in a distorted tetrahedral coordination symmetry ($g_{||} = 2.244$

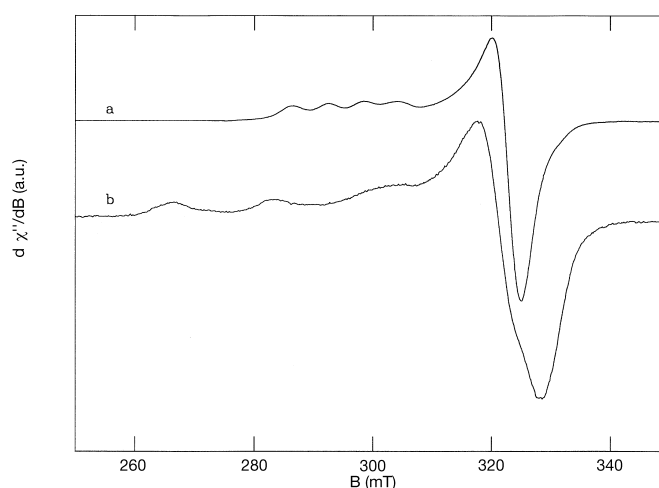


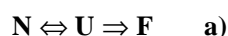
Fig. 7 ESR spectra of PC recorded at 77 K in: a Native state, b Final state

and $A_{||} = 62 \times 10^{-4} \text{ cm}^{-1}$ (Solomon et al. 1992). The low $A_{||}$ value, common to all blue copper proteins (Adman 1993), is ascribed to the widespread delocalization of the unpaired electron in the ligands, in particular the thiolate sulfur of the cysteine residue (Penfield et al. 1985). The high degree of delocalization results from the structure of the copper site.

After thermal transition to the denaturated state, the low temperature spectrum of PC (Fig. 7b) resembles the features of a type II copper complex in a square planar coordination. In fact, $A_{||} = 172 \times 10^{-4} \text{ cm}^{-1}$ is a value characteristic of this kind of geometry (Peisach and Blumberg 1974; den Blaauwen and Canters 1993).

Simulations of the calorimetric profiles

All data collected suggest a denaturation path of the following type for PC:



where N is the native, U the unfolded, and F the final state.

In order to determine the thermodynamic and the kinetic parameters of the two steps in the denaturation process, the experimental curves, obtained at different scan rates (Fig. 2), were fitted with the following equation which simulates the complex process (Milardi et al. 1994):

$$C_{p_{\text{exc}}} = \left[\frac{K\Delta H_U}{(K+1)^2} \left\{ \frac{k}{v} + \frac{\Delta H_U}{RT^2} \right\} + \Delta H_{\text{ag}} \frac{1}{v} \frac{kK}{K+1} \right] \cdot \exp \left\{ -\frac{1}{v} \int_{T_0}^T \frac{kK}{K+T} dT \right\} \quad (6)$$

where K is the thermodynamic equilibrium constant associated with the reversible step,

$$K = \exp \left\{ -\frac{\Delta H_U}{R} \times \left(\frac{1}{T} - \frac{1}{T_{1/2}} \right) \right\} \quad (7)$$

and k is the kinetic constant of the irreversible step,

$$k = \exp \left\{ -\frac{E}{R} \times \left(\frac{1}{T} - \frac{1}{T^*} \right) \right\} \quad (8)$$

ΔH_U is the thermodynamic enthalpy variation associated with the $N \rightleftharpoons U$ unfolding process, E and ΔH_{ag} are the activation energy and the enthalpy associated with the irreversible step respectively, $T_{1/2}$ and T^* are the temperatures at which the thermodynamic equilibrium constant K and the kinetic constant k approach unity, respectively. It must be underlined that the activation energy of the irreversible step is different from E_{app} , obtained by means of Eq. (1). In fact, the relation between E and E_{app} is as follows (Sanchez-Ruiz 1992):

$$E_{\text{app}} = E + \Delta H_U \quad (9)$$

While ΔH_U is a known parameter, ΔH_{ag} , E and T^* can be obtained by fitting the experimental DSC curve with

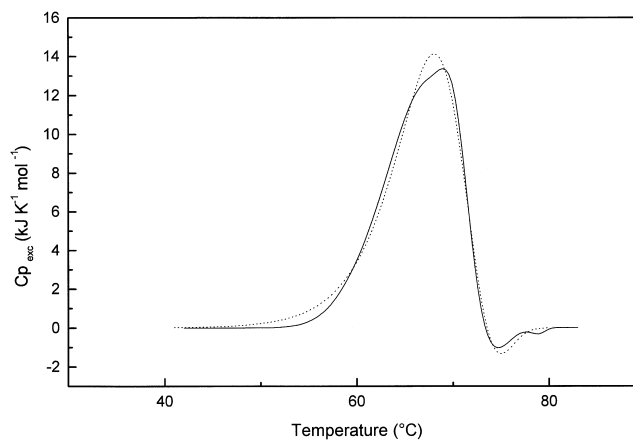


Fig. 8 Curve fitting of the experimental $C_{p_{\text{exc}}}$ profile ($v=0.3^\circ\text{C}/\text{min}$). Equation (6) was used for the fitting program. The optimized parameters are reported in Table 2

Table 2 Kinetic parameters obtained from the fitting of DSC curves carried out at different scan rates as described in the text. Enthalpies and activation energy values are given in kJ/mol, temperature values in $^\circ\text{C}$, scan rates in $^\circ\text{C}/\text{min}$. Minimum increases in the minimization procedure are 1 kJ/mol for enthalpies; 0.1°C for the temperatures. The fixed parameters were: $\Delta H_U = 254 \text{ kJ/mol}$, $T_{1/2} = 69.2^\circ\text{C}$. All the other parameters were floated

v	ΔH_{ag}	E	T^*	M^a	δ^b
0.3	-120	181	79.8	2.1	12.1
0.5	-100	177	80.8	2.8	13.3
0.7	-43	153	85.7	3.1	14.3
1	-72	190	85.8	2.9	15.8

^a $m (\text{kJ K}^{-1} \text{mol}^{-1})$ is a measure of the accuracy of the fitting operation. It is defined as: $m = |\sum_i (C_{p_{\text{theor}}}^i - C_{p_{\text{exp}}}^i) / n|$, where $C_{p_{\text{exp}}}^i$ is the i -th value of the experimental Cp thermogram, $C_{p_{\text{theor}}}^i$ is the corresponding calculated value and n is the total number of points on the scan (the fitting operations were carried out over 100 points)

^b δ is the standard deviation of the $C_{p_{\text{theor}}}^i - C_{p_{\text{exp}}}^i$ function calculation in the denaturation range

Eq. (6) using the SIMPLEX algorithm. In Fig. 8, the experimental profile obtained at $0.3^\circ\text{C}/\text{min}$ is compared with the curve calculated by employing Eq. (6). The parameters used for the simulation of each experimental profile are reported in Table 2. The results show that the fitting parameters are scan rate-dependent. This behavior is ascribable to the fact that the final state, being obtained in an irreversible way, depends on scan rate (La Rosa et al. 1995).

An important requirement in justifying the applicability of the extrapolation procedure and, as a consequence, the goodness of the fitting parameters is the presence of a significant number of molecules in the U state during the thermally induced transition. The relative population of the U state over the entire denaturation range can be calculated by using the following equation (Sanchez-Ruiz 1992):

$$X_U = \frac{K}{K+1} \exp \left\{ -\frac{1}{v} \int_{T_0}^T \frac{kK}{K+1} dT \right\} \quad (10)$$

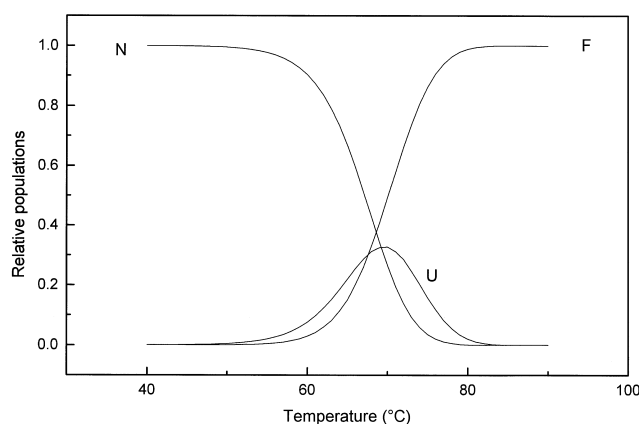


Fig. 9 Relative populations of species N, U and F calculated at 1 °C/min using Eqs. (10) and (11)

The relative populations of species N and F can be calculated with the following equations.

$$X_U / X_N = K, \quad X_N + X_U + X_F = 1 \quad (11)$$

Figure 9 shows the relative populations of the N, U and F species in PC, calculated using Eqs. (10) and (11) and the parameters reported in Table 2. As can be noted the percentage of molecules in the U state at 1 °C/min, (our highest experimental scan rate), is about 20%. This value is considered sufficient to justify the validity of the extrapolation procedure (Freire et al. 1990; La Rosa et al. 1995).

Thermodynamic analysis of the unfolding process

The calculation of the Gibbs free energy for the unfolding process in all the temperature ranges considered requires at least three parameters: ΔH_U , $T_{1/2}$, and ΔC_p . While the first two parameters have already been found, the value of $\Delta C_p = C_{p,U} - C_{p,N}$ cannot be determined experimentally, since the experimental value of C_p at offset temperature is ascribable to the final (F) state and not to the unfolded (U) state. For this reason ΔC_p was calculated on the basis of the Murphy and Gill model (Murphy and Gill 1991). With this model, the value of ΔC_p can be evaluated in terms of the apolar and polar surface exposed to the solvent after the unfolding of PC. The apolar surface is proportional to the number of apolar hydrogen atoms (Jorgensen et al. 1985), while the polar surface is proportional to the number of peptide bonds (Chothia 1976; Privalov and Gill 1988). With this background, the following equations were used for the calculation of ΔC_p :

$$\Delta C_p = \Delta C_{p,ap} + \Delta C_{p,pol} \quad (12)$$

$$\Delta C_{p,ap} = f_{ap} \times N_{CH} \times \Delta C_{p,CH}^0 \quad (13)$$

$$f_{ap} = 0.574 + 0.000702 \times N_{res} \quad (14)$$

$$\Delta C_{p,pol} = 0.73 \times N_{res} \times \Delta C_{p,-CONH-}^0 \quad (15)$$

$$\Delta C_{p,-CH-}^0 = 28 \pm 1 \text{ J/K mol}^{-1} \quad (16)$$

$$\Delta C_{p,-CONH-}^0 = -60 \pm 6 \text{ J/K mol}^{-1} \quad (17)$$

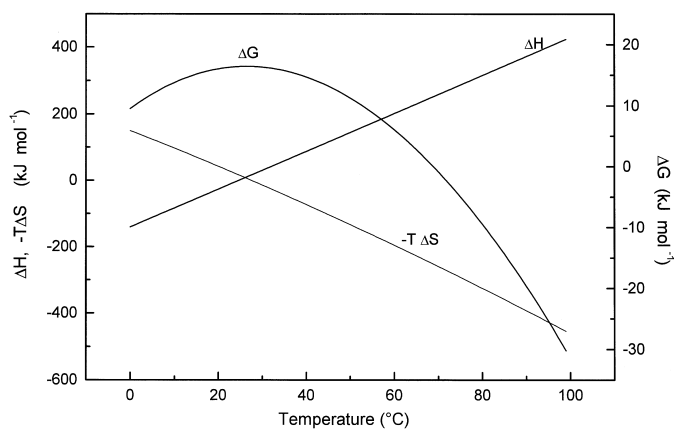


Fig. 10 Temperature dependence of the unfolding Gibbs energy, ΔG , enthalpy, ΔH , and entropy changes, $-T \Delta S$, of PC

where $\Delta C_{p,ap}$ is the denaturational heat capacity change ascribable to apolar groups $\Delta C_{p,pol}$ is the heat capacity change ascribable to polar groups, f_{ap} is the fraction of apolar buried surface area, N_{res} is the number of the residues in the protein, N_{CH} is the number of apolar hydrogen atoms (i. e. the hydrogen atoms directly bound to a carbon atom), $\Delta C_{p,-CH-}^0$ is the specific contribution of a mole of apolar hydrogens to the overall denaturational heat capacity change and $\Delta C_{p,-CONH-}^0$ is the specific contribution ascribable to a mole of residues (Murphy and Gill 1991).

As there are 558 apolar hydrogen atoms and 99 residues in PC (Sykes 1985), ΔC_p is 5.7 kJ K⁻¹ mol⁻¹. By collecting the data obtained and using the following equations:

$$\Delta H(T) = \Delta H_U - \Delta C_p \times (T_{1/2} - T) \quad (18)$$

$$\Delta S(T) = \frac{\Delta H_U}{T_{1/2}} - \Delta C_p \ln \frac{T_{1/2}}{T} \quad (19)$$

$$\Delta G(T) = \Delta H_U \frac{T_{1/2} - T}{T_{1/2}} - \Delta C_p (T_{1/2} - T) + T \Delta C_p \ln \left(\frac{T_{1/2}}{T} \right) \quad (20)$$

it is possible to evaluate ΔG , ΔH and ΔS as a function of temperature (Privalov and Khechinashvili 1974; Privalov 1979, 1990). The results are reported in Fig. 10.

Discussion

The comparison of DSC, ESR and absorbance data made it possible to highlight many fundamental aspects concerning the thermal denaturation of PC. This can be described in terms of two effects of opposite sign. The first is endothermic and related to the unfolding of the protein and the second exothermic step is responsible for the irreversibility of the whole process.

Before comparing DSC and absorbance data, it is worthwhile noting that DSC provides the direct determination of the overall transition properties in the thermally induced structural transitions of proteins (Privalov and Potekhin 1986), whereas the thermodynamic and kinetic variables related to the thermally-induced conformational changes of the active site can be evaluated by following optical density at $\lambda=597$ nm as a function of temperature under the same experimental conditions used for DSC measurements.

The most intriguing aspect of the comparative study of DSC and absorbance results is that the optically-detected thermally induced transition in PC occurs several degrees before the DSC-detected process. The value of the transition temperature, as optically detected, confirms the data of a previous study (Gross et al. 1992) where the thermal transition of PC was investigated by following ellipticity changes at 255 nm as a function of temperature.

In contrast, the enthalpic changes calculated from the extrapolated calorimetric and optical data at infinite scanning rate, are very similar (254 ± 37 kJ/mol in case of DSC analysis, and 284 ± 41 kJ/mol in the case of absorbance data). The similarity between the enthalpy change values suggests that the copper ion plays a crucial role in stabilizing the native conformation of the PC molecule.

The kinetics of the DSC-detected process, as demonstrated by comparing E_a with E_{app} , are different from the kinetics of the optically-detected process. These differences are due both to the different time-response of the experimental techniques and to the different nature of the physical transitions monitored by the two techniques. In fact, the OD transition is related to the Cys \rightarrow Cu⁺⁺ charge transfer absorption, which is primarily responsible for the absorbance at 597 nm. This absorption depends on the geometry of the atoms belonging to the first coordination sphere of the copper ion, and thus on the secondary and tertiary structure of the protein.

On the other hand, DSC-detected transitions are related to the overall conformational changes of the whole protein molecule. The time scale of the last thermally-induced change is presumably slower than the optical transition.

Thermodynamic stability of PC

Using the equations proposed by Murphy and Gill (1991), we can calculate the contributions of the polar and apolar components of the protein to the thermodynamic functions for unfolding.

In particular, the apolar contribution to the protein entropy change, ΔS , is given by:

$$\Delta S_{ap} = \Delta C_{p,ap} \ln (T/385) \quad (21)$$

The remaining entropy change per residue is the entropy change common to every residue in the protein and reflects the configurational contribution of the peptide group when exposed to water:

$$\Delta S_{conf} = 18.1 \times N_{res} + \Delta C_{p,pol} \ln (T/385) \quad (22)$$

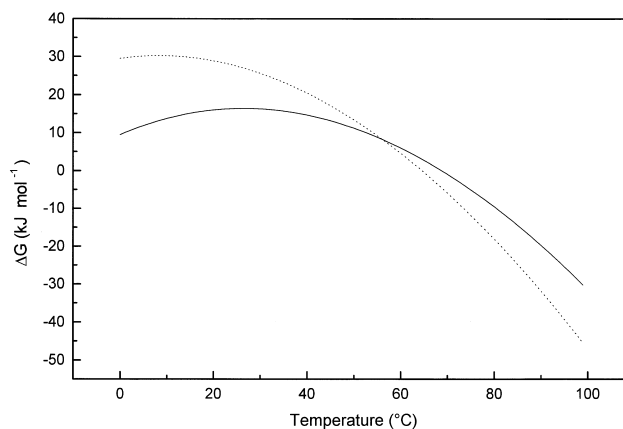


Fig. 11 Gibbs energy denaturational changes of PC. The *dotted curve* represents the expected behavior in terms of Murphy and Gill's model. The *solid line* is the experimental Gibbs energy function calculated with Eq. (20)

The apolar contribution to protein denaturational enthalpy can be expressed as follows:

$$\Delta H_{ap} = \Delta C_{p,ap} \times (T - 373.6) \quad (23)$$

While, the polar contribution to the protein enthalpy change is estimated as follows:

$$\Delta H_{pol} = 5.64 \times N_{res} + \Delta C_{p,pol} \times (T - 373.6) \quad (24)$$

The overall free energy change for protein unfolding is then given in terms of the various enthalpic and entropic terms described above:

$$\Delta G = \Delta H_{pol} - T \Delta S_{conf} + \Delta G_{ap} \quad (25)$$

where

$$\Delta G_{ap} = \Delta C_{p,ap} \left[(T - 373.6) - T \ln \left(\frac{T}{385} \right) \right] \quad (26)$$

In Fig. 11 the experimental ΔG function related to the thermal unfolding of PC is compared with the expected ΔG function calculated for a hypothetical protein with the amino-acid composition of PC using Eq. (25).

We must remember at this point that the model proposed by Murphy and Gill considers the contributions of metal ions and/or disulfide bridges to the thermodynamic properties of proteins to be negligible. In fact, in their model the average structural features of proteins are considered only in terms of polar and apolar groups. This consideration suggests that the metal ion is probably responsible for the differences between the experimental and the thermodynamic functions calculated by means of Eq. (25).

As can be noted, the experimental and the expected ΔG functions have the same value at $T = 56$ °C. At $T > 56$ °C the experimental ΔG function is greater than the calculated one. An opposite effect is observed at $T < 56$ °C.

This behavior can be explained by considering that enthalpic contributions are stabilizing at high temperature and destabilizing at low temperatures (Fig. 10). In contrast, entropic contributions are stabilizing at low temperatures and destabilizing at high temperatures. These considera-

tions would suggest that the stabilization of the native state of PC induced by the copper ion has an enthalpic rather than entropic character. The resulting stability of PC is very low, especially if compared to that of azurin, which also contains a copper ion in the active site. (La Rosa et al. 1995; Engeseth and McMillin 1986). This result can be explained if we consider the reduced size of PC (99 residues against 128) and the presence of a disulfide bond (Cys3–Cys26) in azurin. In fact, intramolecular disulfide bonds in protein molecules have been shown to increase protein stability significantly (Pace et al. 1988; Ladbury et al. 1994).

Acknowledgements R. G. thanks the University of Calabria for a post-doctoral fellowship. This work was partially supported by MURST (Ministero della Ricerca Scientifica e Tecnologica), CNR (Consiglio Nazionale delle Ricerche), INFN (Istituto di Fisica della Materia) and CIB (Consorzio Interuniversitario Biotecnologie).

References

- Adman ET (1993) Copper protein structures. *Adv Prot Chem* 42: 145–197
- Adman ET (1985) Structure and function of small blue copper proteins. In: Morrison PM (ed) *Topics in molecular and structural biology: metalloproteins*, vol 6, part 1. Chemie, Weinheim, pp 1–42
- Biltonen R, Freire RL (1978) Thermodynamic characterization of conformational states of biological macromolecules using differential scanning calorimetry. *CRC Crit Rev Biochem* 5: 85–124
- Chazin WJ, Wright PE (1988) Complete assignment of the ¹H nuclear magnetic resonance spectrum of French bean plastocyanin. Sequential resonance assignments, secondary structure and global fold. *J Mol Biol* 202: 623–636
- Chothia C (1976) The nature of accessible and buried surface in proteins. *J Mol Biol* 105: 1–14
- Colman PM, Freeman HC, Guss JM, Murata M, Norris VA, Ramshaw JAM, Venkatappa MP (1978) X-ray crystal structure analysis of plastocyanin at 2.7 Å resolution. *Nature* 272: 319–324
- Connelly P, Ghosaini L, Hu CQ, Kitamura S, Tanaka A, Sturtevant JM (1991) Differential scanning calorimetric study of the thermal unfolding of seven mutant forms of phage T4 Lysozyme. *Biochemistry* 30: 1887–1895
- den Blaauwen T, Canters GW (1993) Creation of Type-1 and Type-2 copper sites by addition of exogenous ligands to the pseudomonas *Aeruginosa* azurin His117Gly mutant. *J Am Chem Soc* 115: 1121–1129
- Dill KA, Shortle D (1991) Denaturated states of proteins. *Annu Rev Biochem* 60: 795–825
- Edge V, Allewell NM, Sturtevant JM (1985) High resolution differential scanning calorimetric analysis of the subunits of *E. coli* aspartate transcarbamoylase. *Biochemistry* 24: 5899–5906
- Engeseth HR, McMillin DR (1986) Studies of thermally induced denaturation of azurin derivatives by differential scanning calorimetry: evidence for copper selectivity. *Biochemistry* 25: 2448–2455
- Freire E, Biltonen RL (1978) Statistical thermodynamics of thermal transitions in macromolecules I. Theory and application to homogeneous systems. *Biopolymers* 17: 463–479
- Freire E, Van Odsol WW, Mayorga OL, Sanchez-Ruiz JM (1990) Calorimetrically determined dynamics of complex unfolding transitions in proteins. *Annu Rev Biophys Chem* 19: 159–188
- Galisteo ML, Sanchez-Ruiz JM (1993) Kinetic study into the irreversible thermal denaturation of bacteriorhodopsin. *Eur Biophys J* 22: 5–30
- Gewirth AA, Solomon EI (1988) Electronic structure of plastocyanin: excited state spectral features. *J Am Chem Soc* 110: 3811–3819
- Gray HB, Solomon I (1981) Electronic structures of the blue copper centers in proteins. In: Spiro T (ed) *Copper proteins*. Wiley, New York, pp 1–39
- Gross EL, Draheim JE, Curtiss AS, Crombie B, Scheffer A, Pan B, Chiang C, Lopez A (1992) Thermal denaturation of plastocyanin: the effect of oxidation state, reductants and anaerobicity. *Arch Biochem Biophys* 298: 413–419
- Guss JM, Freeman HC (1983) Structure of oxidized poplar plastocyanin at 1.6 Å resolution. *J Mol Biol* 169: 521–563
- Guss JM, Harrowell PR, Murata M, Norris VA, Freeman HC (1986) Crystal structure analysis of reduced poplar plastocyanin at six pH values. *J Mol Biol* 192: 361–373
- Guss JM, Bartunik HD, Freeman HC (1992) Accuracy and precision in protein structure analysis: restrained least-squares refinement of the structure of poplar plastocyanin at 1.33 Å resolution. *Acta Cryst B* 48: 790–811
- Guzzi R, La Rosa C, Grasso D, Milardi D, Sportelli L (1996) An experimental model for the thermal denaturation of azurin: a kinetic study. *Biophys Chem* 60: 29–38
- Hernandez-Arana A, Rojo-Dominguez A, Altamirano MM, Calcagno ML (1993) Differential scanning calorimetry of irreversible denaturation of *Escherichia coli* glucosamine-6-phosphate deaminase. *Biochemistry* 32: 3644–3648
- Jorgensen WL, Gao J, Ravimohan C (1985) Monte carlo simulations of alkanes in water: hydration numbers and the hydrophobic effect. *J Phys Chem* 89: 3470–3473
- Ladbury JE, Kishore N, Hellinga HW, Wynn R, Sturtevant JM (1994) The thermodynamics of formation of a three-strand DNA three way junction complex. *Biochemistry* 33: 3688–3692
- La Rosa C, Milardi D, Grasso D, Guzzi R, Sportelli L (1995) Thermodynamics of the thermal unfolding of azurin. *J Phys Chem* 99: 14864–14870
- Merchant S, Bogorad L (1986a) Regulation by copper of the expression of plastocyanin and cytochrome c552 in *Chlamydomonas reinhardtii*. *Mol Cell Biol* 6: 462–469
- Merchant S, Bogorad L (1986b) Rapid degradation of apoplastocyanin in Cu(II)-deficient cells of *Chlamydomonas reinhardtii*. *J Biol Chem* 261: 15850–15853
- Milardi D, La Rosa C, Grasso D (1994) Extended theoretical analysis of irreversible thermal protein unfolding. *Biophys Chem* 52: 183–189
- Murphy KP, Gill SJ (1991) Solid model compounds and the thermodynamics of protein unfolding. *J Mol Biol* 222: 699–709
- Pace CN, Grimsley GR, Thomson JA, Barnett BJ (1988) Conformational stability and activity of ribonuclease T1 with zero, one and three intact disulfide bonds. *J Biol Chem* 263: 11820–11825
- Peisach J, Blumberg WE (1974) Structural implication derived from the analysis of electron paramagnetic resonance spectra of natural and artificial copper proteins. *Arch Biochem Biophys* 15: 691–708
- Penfield KW, Gewirth AA, Solomon EI (1985) Electronic structure and bonding of the blue copper site in plastocyanin. *J Am Chem Soc* 107: 4519–4529
- Poklar N, Vesnaver G, Lapanje S (1993) Studies by UV spectroscopy of thermal denaturation of β -lactoglobulin in urea and alkyl-urea solutions. *Biophys Chem* 47: 143–151
- Privalov PL, Gill SJ (1988) Stability of protein structure and hydrophobic interactions. *Adv Prot Chem* 39: 191–234
- Privalov PL, Khechinashvili NN (1974) A thermodynamic approach to the problem of stabilization of globular protein structure: a calorimetric study. *J Mol Biol* 86: 665–684
- Privalov PL, Potekhin SA (1986) Scanning microcalorimetry in studying temperature induced changes in proteins. *Methods Enzymol* 4: 4–51
- Privalov PL (1979) Stability of proteins. *Adv Prot Chem* 33: 167–239
- Privalov PL (1990) Thermodynamic bases of the stability of protein structure. *Therm Acta* 163: 33–46
- Redimbo MR, Yeates TO, Merchant S (1994) Plastocyanin: structural and functional analysis. *J Bioenerg Biomemb* 26: 49–66
- Sanchez-Ruiz JM (1992) Theoretical analysis of Lumry-Eyring models in differential scanning calorimetry. *Biophys J* 61: 921–935

- Sanchez-Ruiz JM, Lòpez-Lacomba J, Cortijo M, Mateo PL (1988) Differential scanning calorimetry of the irreversible thermal denaturation of thermolysin. *Biochemistry* 27: 1648–1652
- Sanderson DG, Anderson LB, Gross EL (1986) Determination of the redox potential and diffusion coefficient of the protein plastocyanin using optically transparent filar electrodes. *Biochim Biophys Acta* 852: 269–278
- Solomon EI, Baldwin MJ, Lowery MD (1992) Electronic structures of active sites in copper proteins: contributions to reactivity. *Chem Rev* 92: 521–542
- Sturtevant JM (1987) Biochemical applications of differential scanning calorimetry. *Annu Rev Phys Chem* 38: 463–512
- Sykes AG (1991) Active-site properties of the blue copper proteins. *Adv Inorg Chem* 36: 376–408
- Sykes AG (1985) Structure and electron-transfer reactivity of the blue copper protein plastocyanin. *Chem Soc Rev* 14: 283–315
- Wang CX, Giugliarelli G, Cannistraro S, Fini C (1986) Spectroscopic and computer simulation study on paramagnetic copper-containing plastocyanin. *Il Nuovo Cimento D* 8: 76–90